Bull. Mater. Sci., Vol. 39, No. 1, February 2016, pp. 91–96. © Indian Academy of Sciences.

The enhanced interface effect induced by thermal pressure in $Nd_{0.7}Sr_{0.3}MnO_y$ ceramics

SHUNSHENG CHEN[1,2], DAWEI SHI[2], SHAOZHEN LI[1], CHANGPING YANG[2,*] and YALI ZHANG[3]

[1]Institute for Quantum Materials and School of Mathematics and Physics, Hubei Polytechnic University, Huangshi 435003, PR China

[2]Hubei Collaborative Innovation Center for Advanced Organic Chemical Materials, Faculty of Physics & Electronic Science, Hubei University, Wuhan 430062, PR China

[3]Xinyang Vocational & Technical College, The School of Mathematics and Computer Science, Xinyang 464000, PR China

MS received 28 October 2014; accepted 7 September 2015

Abstract. **Polycrystalline ceramics $Nd_{0.7}Sr_{0.3}MnO_y$ prepared by solid-state reaction were treated under high pressure of 9 GPa and temperature of 1000 K. The electrical transport behaviour of samples were investigated by a variable temperature system and a peculiar transport character was found at low temperature of 120 K, the *I–V* showed an obvious step-shape behaviour with the increase in the measurement voltages; at much lower temperature of 12.3 K, the *I–V* curves exhibited a notable symmetric hysteresis at a critical voltage of 4.5 V, although a linear *I–V* behaviour at 293 K. On the other hand, the *R–T* measurement revealed that the resistivity peak (resistivity at T_{MI}) disappeared gradually and is replaced by a resistivity platform with the increase in the load currents, surprisingly, the resistivity platform broadened with continuous increase in the load currents but weakened when an external magnetic field was applied. All of these phenomena were not observed for the un-treated sample. The particle attenuated and the enhanced interface effect which resulted from the violent thermal-pressure treatment was responsible for the unique electromagnetic transport.**

Keywords. **Thermal-pressure treatment; interfacial effect; electrical/magnetic transport; microstructure; manganites.**

1. Introduction

The alkali-earth-doped perovskite-type manganites $R_{1-x}D_xMnO_3$ (R—rare earth, D—alkali earth elements) have drawn remarkable interests due to the rich physics from interactions among spin, charge, lattice, and orbital degrees of freedom as well as the potential applications in industry such as colossal magnetoresistance (CMR), colossal electroresistance (CER) and electric-pulse-induced resistance switching (EPIR) effects [1–5]. Basically, the manganites are strong correlated electronics system, and the electromagnetic transport is greatly influenced by the external disturbances such as electric/magnetic fields, radiation, temperature, illumination, doping, thermal-pressure and so on [6–9]. Besides these factors mentioned above, it is also reported that the microstructure defects, grain/phase boundaries, and various inhomogeneous factors are closely related to the transport properties of manganites due to the resistivity is the structure-sensitive parameters [10], and can induce various novel effects as interface-dependent ER effect, MR effect [11,12], EPIR effect [13–15] and low field magnetoresistance (LFMR) effect [16,17].

For the NdSrMnO system with doping ratio $x = 0.3$, $Nd_{0.7}Sr_{0.3}MnO_y$ generally exhibits an optimal double exchange interaction (DE) accompanied with the Curie temperatures of 229–239 K, and the electromagnetic transport is comprehensively investigated [18–24]. In this work, an unusual electrical transport behaviour is observed in the NSMO ceramics prepared by solid-state reaction and sequentially thermal-pressure treatment. The peculiar *I–V* and *R–T* character may mainly result from the enhanced interface effects.

2. Experimental

Polycrystalline $Nd_{0.7}Sr_{0.3}MnO_y$ with perovskite structure was prepared using the conventional solid-state reaction method. High-purity powders of Nd_2O_3, $SrCO_3$ and MnO_2 were used as raw materials. Nd_2O_3 and $SrCO_3$ were pretreated at 1173 K for 6 h and 673 K for 4 h, respectively, before mixing. The samples from solid-state reaction were sequentially treated under 9 GPa static pressure and high temperatures of 1000 K for 100 s and rapidly decreased to 80 K in 10 min. Figure 1 shows the diagrammatic sketch of thermal-pressure device. The closet space for samples is no more than

*Author for correspondence (cpyang@hubu.edu.cn)

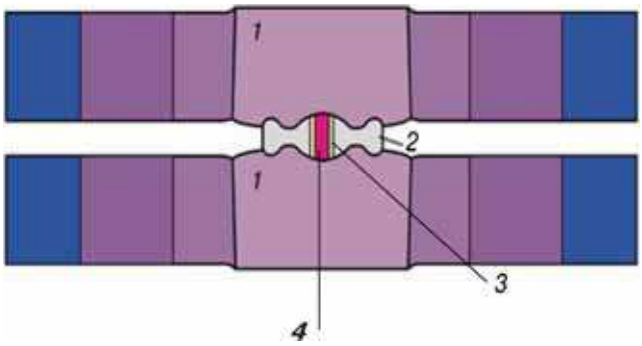

Figure 1. Diagrammatic sketch of section for thermal-pressure device. 1: Toroid-type camera, 2: plunger, 3: transmitting medium and 4: sample.

0.1 cm^3, and the details of sample preparation can be found in other works [25]. Powder X-ray diffraction (DRON-3, Cu-Kα, Japan) are used to identify the phase purity. Four parallel bar electrodes with 1.2 mm spacing are fabricated regularly on side of sample using Ag-paint. The field-emission scanning electronic microscope (FESEM) is used to investigate the microstructure of sample before and after thermal-pressure treatment. The *I–V* and *R–T* are measured using a Keithley 2400 multimeter with a computer-controlled program. Thermomagnetic curves (*M–T*) were measured using a vibrating sample magnetometer (VSM) in a field cooling at 1000 Oe. For convenience, the samples before and after thermal-pressure treatment are named No. 1 and No. 2, respectively.

3. Results and discussion

Figure 2 shows X-ray diffraction (XRD) patterns of No. 2. For comparison, the XRD patterns of No. 1 is also given in the inset of figure 1. It clearly shows that No. 2 remains the same orthorhombic perovskite structure with Pnma space group as No. 1 although undergoes a violent thermal-pressure process, indicating no impurity phase introduces under the thermal-pressure treatment. But there are some changes in the MnO_6 octahedra for No. 2, just seen from table 1, the *a*, *b*, *c* and *V* parameters have changed only slightly, but there are quite noticeable changes in the Mn–O(1) and Mn–O(2) bond lengths, especially the Mn–O(1)–Mn and Mn–O(2)–Mn bond angles, which will produce a complex local deformation of the MnO_6 octahedra.

Figure 3 shows *I–V* measurement results under given temperatures for No. 1 and No. 2, respectively. From figure 3 three remarkable points can be found: one is that for No. 1 the *I–V* exhibits linear transport behaviour at all of three given temperatures 293, 120 and 13 K, and these *I−V* curves well coincide with each other whether loading the magnetic field of 1 T or not, indicating that no ER and MR effects occur (see figure 3d–f), this is in agreement with that reported in the earlier study [26]. However, for No. 2, it is not the case that a large MR behaviour appears at low temperatures of 120 and 12.3 K, though it is also linear character at 293 K. The

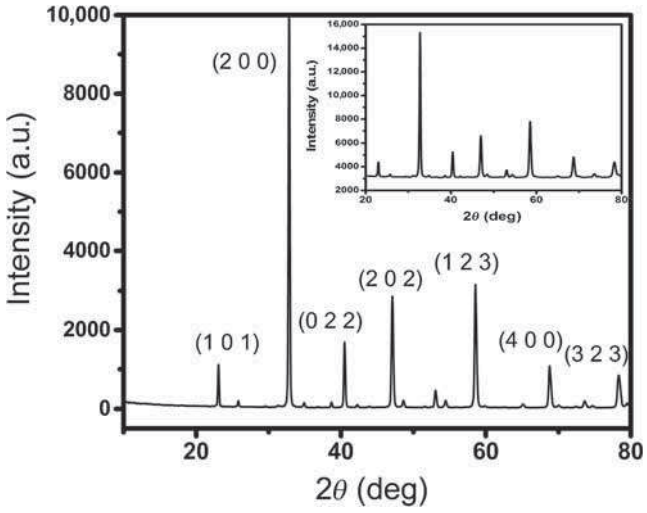

Figure 2. X-ray pattern of No. 2 and No. 1 (inset) samples.

MR effect at low temperature is usually ascribed to the interfacial effects [17], for sample No. 2, it may possess much larger volume of interface than that of sample No. 1. Secondly, the *I-V* curves at low temperatures (120, 12.3 K) show an obvious step shape when the applied voltage is higher than a critic voltage *V*c, for example $V\mathrm{c} = 5.16$ V at 120 K, and $V\mathrm{c} = 4.81$ V at 12.3 K, respectively, indicating a critic voltage-related ER behaviour. From figure 3b, the MR values of 22.7 and 19% can be obtained under 1 T magnetic field when applied voltages are $V < V\mathrm{c}$ and $V > V\mathrm{c}$, respectively. Here, MR is defined as $\mathrm{MR} = [(R_0 - R_\mathrm{H})/R_0]{*}100\%$ (R_0, R_H are the resistances under magnetic field of 0 and 1 T, respectively), in the same way, the MR value of 15.2% ($V < V\mathrm{c}$) and 13.7% ($V > V\mathrm{c}$) at 12.3 K is also obtained. The third is that at 12.3 K the *I–V* curves exhibit a clear and symmetric hysteresis (see the inset of figure 3c) and they disappear when a magnetic field is applied with 1 T. Generally, the electrical transport property of a material is characterized by the *I–V* measurements. For uniform materials, these measuring results are strongly relied on the lattice vibrations (phonons) and the scattering of impurity ions, so the *I–V* can follow Ohm's law; however, for non-uniform materials, the *I–V* curve usually exhibits nonlinear and hysteretic property due to various impurities and disorders unavoidably exist. Experimentally, the Joule heat can also produce irregular nonlinearity and/or hysteresis *I–V* [3,27]. In this case, the *I–V* measuring rate is 0.05 V s^{-1}, and the interval between every point is 2 s. The hysteretic *I–V* curves are measured tens of times at different periods and they always well repeat, indicating that the hysteresis do not origin from the Joule heat effect. Additionally, the compliance current is 1.05 A for the *I–V* measurement for both of samples, so there are different voltage scanning areas due to the different resistivity for the two samples.

In order to investigate the transport behaviour of No. 2 in more depth, we examine the resistivity dependence of temperature with different loading electric currents (2, 3 mA) and magnetic fields (0, 1 T), for comparison, the *R–T* curves

Table 1. Unit cell parameters of samples No. 1 and No. 2.

Samples	Unit cell parameters (Å)				MnO_6 parameters (nm)				
	a	*b*	*c*	*V*	Mn–O(1)	Mn–O(2)	Mn–O(2)	Mn–O(1)–Mn	Mn–O(2)–Mn
No. 1	5.4461	7.7116	5.4680	230.66	1.97(1)	1.90(7)	2.02(8)	156.5(33)	161.0(20)
No. 2	5.4668	7.7102	5.4709	230.69	2.01(1)	1.89(7)	2.01(7)	147.4(23)	165.8(16)

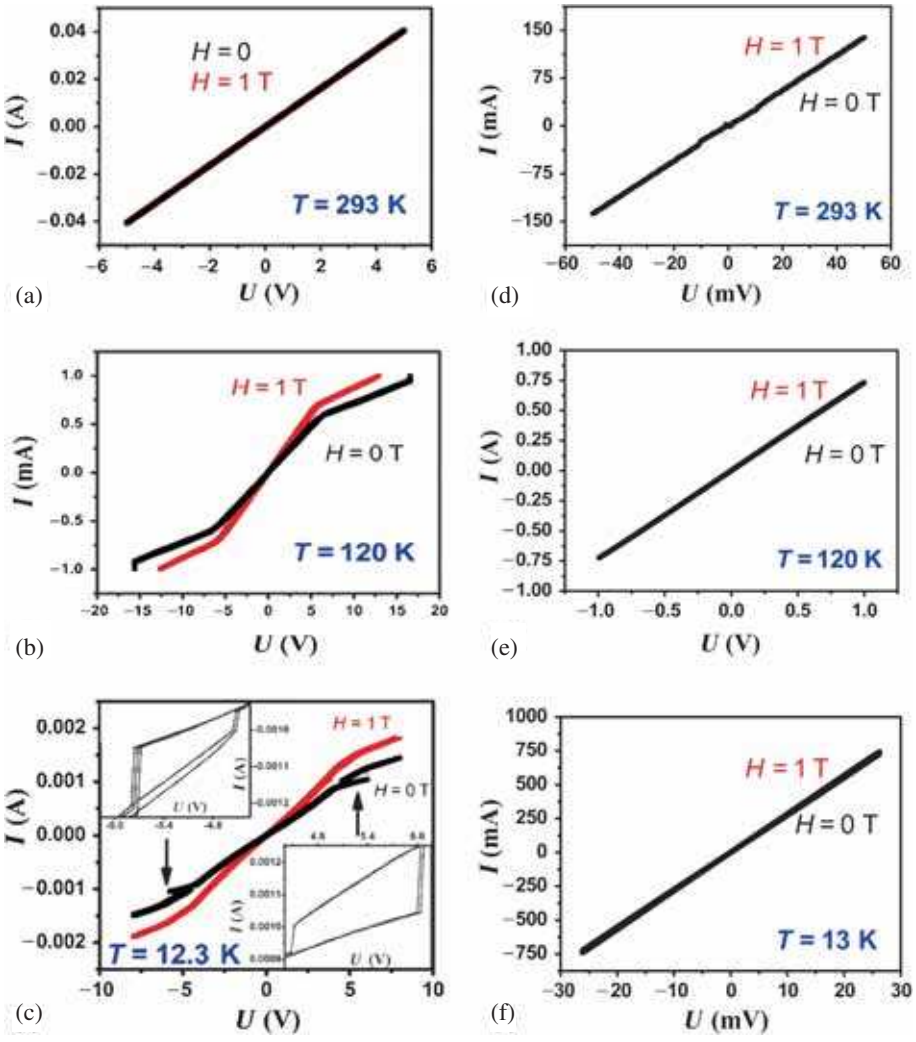

Figure 3. *I–V* characteristics of No. 2 (**a**, **b**, **c**) and No. 1 (**d**, **e**, **f**) at given temperatures 293, 120 and 12.3 K, respectively.

of No. 1 under the same measuring condition are also given, as shown in figure 4. The resistivity peak at T_{MI} corresponds to a transition between a ferromagnetic metallic state and a paramagnetic isolating state [24]. For No. 2, the T_{MI} is about 121 K, which is 100 K lower than that of No. 1 ($T_{MI} = 223$ K) (see figure 4). However, an interesting thing is that they do not generate resistivity peak but a resistivity platform, and the width of platform broadens with the increase in load current from 2 to 3 mA. Similar to the results observed in other manganites [2,12,23,26], the resistivity also decreases with the increase in the load currents, indicating that an ER effect happens. More curiously, the resistivity platform disappears and returns to a resistivity peak when a magnetic field of 1 T is applied to the sample under the same current of 2 mA (see figure 4a). On the other hand, the resistivity of No. 2 is about four orders of magnitude higher than that of No. 1. The large resistivity and the peculiar transport behaviour are frequently attributed to the microstructure defects and magnetic moment disorders [28,29], which usually leads to the decrease of metal–insulator transition temperature T_{MI} [30].

In order to clarify magnetic property of the two samples, the magnetization dependences of temperatures are investigated and the results are shown in figure 5. For sample No. 1, the saturated magnetization decreases sharply with the increase in temperature and the value of T_C 220 K can be

easily obtained from the slope of M–T curves. However, for the thermal treatment sample No. 2, the saturated magnetization decreases slowly and the T_C is only 123 K. It is known that the width of the FM–PI transition is a microstructure-sensitive property, as it is defined by atomic, spin and structural inhomogenities, which are always present in polycrystals, especially in samples with larges of interfaces. For No. 2, the volume of the intergranular layers increase, which contain a large amount of structural defects and distortions, and lead to a weakening of ferromagnetic Mn–O–Mn coupling, and then some manganese magnetic moments are ordered antiferromagnetically or frustrated due to amorphization.

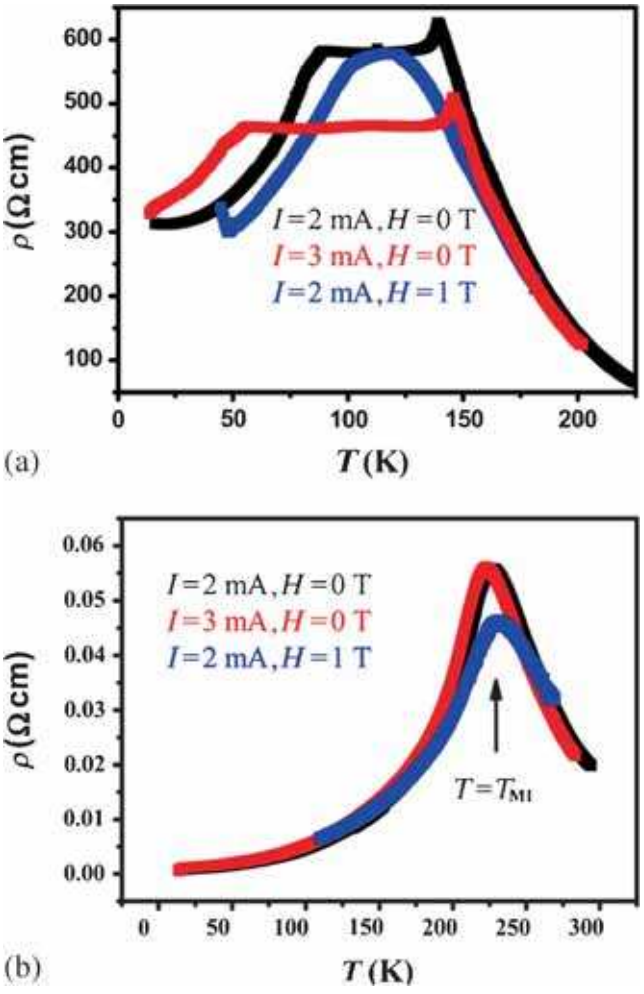

Figure 4. Temperature dependence of the resistivity of (**a**) No. 2 and (**b**) No. 1.

In order to verify the effect of microstructure on the electrical transport, the microstructures of No. 1 and No. 2 were examined and is as shown in figure 6. For No. 1, the crystalline grains were clearly visible and edge sharpness was found with the average grain size is about 1.1 μm. Besides, many more pores with uniform size in volume can also be seen (see figure 6a). These pores are usually formed in the period of sintering due to the different crystallizing processes of grains. In stark contrast to No. 1 is that, however, the grains of No. 2 are much more compact and small. Obviously, the grain size is only about 0.4 μm on average and few pores can be seen. These grains could be split as much smaller grains under large pressure and high temperatures, and form many more blurred and disordered grain boundaries (see figure 6b). It is reasonable to regard that, for No. 2, there are plenty of electromagnetically and structurally non-uniform factors exist, thus, a magnetically and/or electrically related built-in electric field would forms, and its barriers height can be regulated by the external electric and magnetic fields. Hence a remarkable ER or MR effect is expected to occur by lowering the potential of barrier or re-arraying the moments when applying an external electrical or magnetic field to the sample. This is similar to that found in $Nd_{0.7}Sr_{0.3}MnO_3$ ceramics prepared by the ball-milling method, in which a screw dislocation like is responsible for the resistivity changing [26].

Basically, the property of electrical transport for a certain solid-state material is rest with the carriers' moving from one location to another in orientation. Hence, the resistivity is intensely dependent on the surroundings of carriers around such as the route of carrier's moving, the physical properties of materials and the homogeneity of distribution of the medium. Actually, in the manganites system the electrical transport is highly influenced by the interfacial effect (such

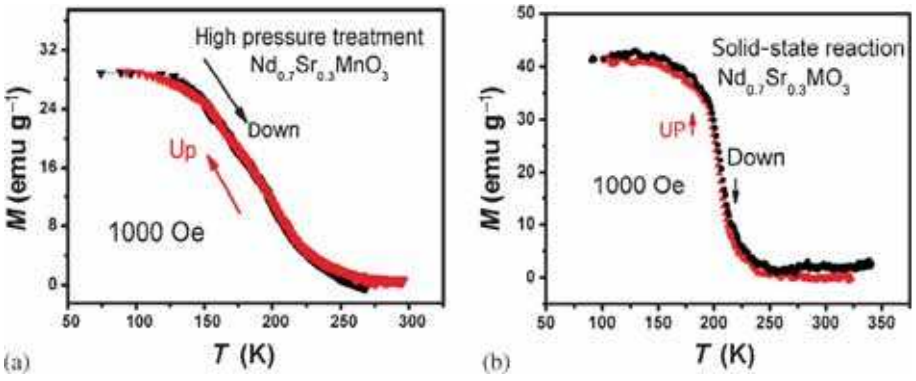

Figure 5. Magnetization dependence of temperature of (**a**) No. 2 and (**b**) No. 1.

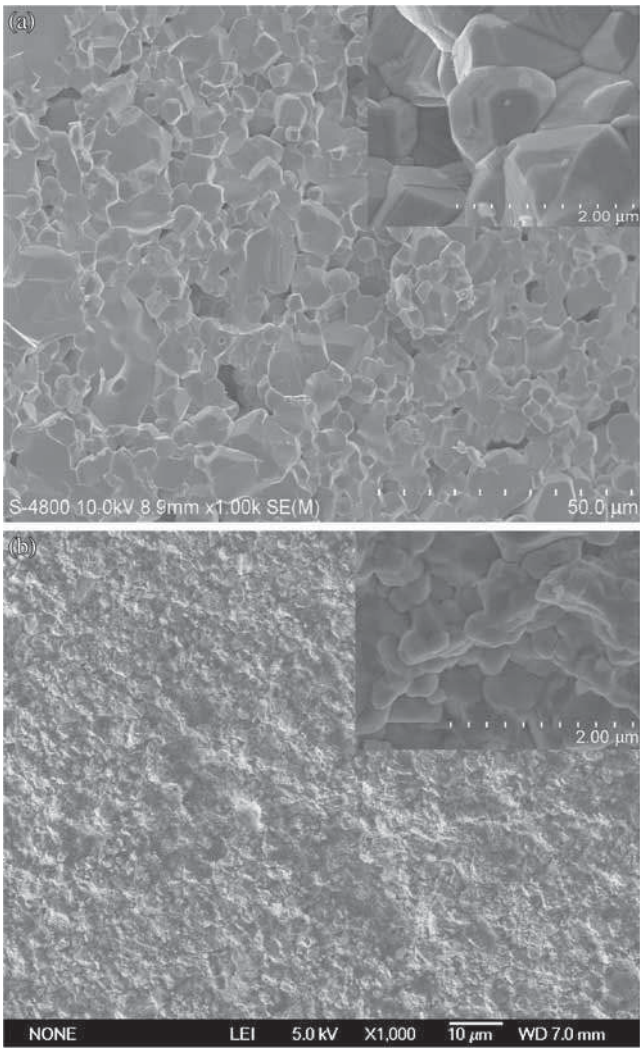

Figure 6. SEM image of (**a**) No. 1 sample and (**b**) No. 2 sample.

as grain boundaries, electrode-bulk interfaces and so on), and the space charge effects are responsible for their physics. So, for the sample treated by thermal pressure, finer grains, compacter boundaries, more defects, and impurity ions segregated preferentially at the boundaries would build up much more obstacles and hinder the carriers' moving, which leads to more larger resistivity, although the MnO_6 octahedra also deformed in this case. On the other hand, the step shape and resistivity platform behaviours mentioned above could be related to the collapse of built-in electric field in local under external electric field, and the magnetic field facilitates the moment arrangement thus improves the transport environment of carriers, decrease the resistivity so as to produce the MR at low temperatures, yet, the detailed interaction process and physics still need the further investigation.

4. Conclusions

In summary, polycrystalline ceramics $Nd_{0.7}Sr_{0.3}MnO_y$ were prepared by solid-state reaction and post-treated by the pressure of 9 GPa and temperature of 1273 K. The thermal-pressure treatment leads to the tinier grains and then enhanced the interface effects, which strongly influences the carriers' moving and result in the step-shape $I-V$ at 120 K and the hysteretic $I-V$ at lower temperature 12.3 K. The peculiar electric transport behaviour is also reflected by the R–T measurement that an unusual resistivity platform broaden with the increase in the loading current but weaken if applying an external magnetic field on the sample, for the aim of understanding the physics of electric transports of thermal treated samples, the further investigation is necessary.

Acknowledgements

We thank the Project of the Educational Commission of Hubei Province (No. B2014025), the Natural Science Foundation of Hubei Province (No. B2014068), the Natural Science Foundation of China (No. 51302074), and Hubei Polytechnic University (No. 12xjz01R) for their financial supports.

References

[1] Chen X G, Ma X B, Yang Y B, Chen L P and Xiong G C 2011 *Appl. Phys. Lett.* **98** 122102
[2] Yang C P, Chen S S, Zhou Z H, Xu L F, Wang H, Hu J F, Morchshakov V and Bärner K 2007 *J. Appl. Phys.* **101** 063909
[3] Yu C Y, Feng P and Fei Z 2010 *N. J. Phys.* **12** 023008
[4] Quintero M, Levy P, Leyva A G and Rozenberg M J 2007 *Phys. Rev. Lett.* **98** 116601
[5] Liu S Q, Wu N J and Ignatiev A 2000 *Appl. Phys. Lett.* **76** 2749
[6] Moritomo Y, Kuwahara H, Tomioka Y and Tokura Y 1997 *Phys. Rev. B* **55** 7549
[7] Kozlenko D P, Goncharenko I N, Savenko B N and Voronin V I 2004 *J. Phys.: Condens. Matter* **16** 6755
[8] Acha C, Garbarino G and Leyva A G 2007 *Physica B* **398** 212
[9] Miyano K, Tanaka T, Tomioka Y and Tokura Y 1997 *Phys. Rev. Lett.* **78** 4257
[10] Chen S S, Yang C P, Kan Z L, Medvedeva I V and Marchenkov S 2012 *Acta Phys. Sin.* **61** 186202
[11] Xie Y W, Sun J R, Wang D J, Liang S and Shen B G 2006 *J. Appl. Phys.* **100** 033704
[12] Chen S S, Yang C P, Wang H, Medvedeva I V and Bärner K 2010 *Mater. Sci. Eng. B* **172** 167
[13] Shang D S, Wang Q, Chen L D, Dong R, Li X M and Zhang W Q 2006 *Phys. Rev. B* **73** 245427
[14] Dong R, Wang Q, Chen L D, Shang D S, Chen T L, Li X M and Zhang W Q 2005 *Appl. Phys. Lett.* **86** 172107
[15] Yang C P, Chen S S, Dai Q and Song X P 2011 *Acta Phys. Sin.* **60** 117202
[16] Li X W, Gupta A, Xiao G and Gong G Q 1997 *Appl. Phys. Lett.* **71** 1124
[17] Wang K F and Liu J M 2003 *Prog. Phys.* **23** 192
[18] Hsu Daniel, Lin J G and Wu W F 2007 *J. Magn. Magn. Mater.* **310** 978

[19] Ying Y, Fan J Y, Pi L, Hong B, Tan S and Zhang Y H 2007 *Solid State Commun.* **144** 300

[20] Venkatesh R, Sethupathi K, Pattabiraman M and Rangarajan G 2007 *J. Magn. Magn. Mater.* **310** 2813

[21] Krishnamoorthy C, Sethupathi K, Sankaranarayanan V, Nirmala R and Malik S K 2007 *J. Magn. Magn. Mater.* **308** 28

[22] Chen S S, Luo X J, Shi D W, Li H and Yang C P 2013 *J. Mater. Sci. Technol.* **29** 737

[23] Chen S S, Wang R L, Wang H and Yang C P 2010 *J. Rare Earths* **28** 251

[24] Chen S S, Yang C P and Luo X J 2012 *Chin. Phys. Lett.* **29** 027302

[25] Medvedeva I V, Dyachkova T, Tyutyunnik A, Zaynulin Yu, Marchenkov V, Marchenkova E, Yang C P, Chen S S and Baerner K 2011 *Solid State Phenom.* **168–169** 39

[26] Chen S S, Yang C P and Dai Q 2010 *J. Alloys Compd.* **491** 1

[27] Yan Z B, Wang K F, Li S Z, Luo S J and Liu J M 2009 *Appl. Phys. Lett.* **95** 143502

[28] Das D, Saha A, Russek S E, Raj R and Bahadur D 2003 *J. Appl. Phys.* **93** 8301

[29] Petrov D K, Krusin-Elbaum L, Sun J Z, Feild C and Duncombe P R 1999 *Appl. Phys. Lett.* **75** 995

[30] Chen S S, Yang C P, Zhou Z H, Guo D H, Wang H and Rao G H 2008 *J. Alloys Compd.* **463** 271